

# Development of a machine learning model to determine the forces on the piston in the pump-tube of a two-stage gas gun deforming due to a taper

Benjamin Alheit<sup>\*1, 2</sup>

<sup>1</sup>*Centre for Research in Computational & Applied Mechanics, University of Cape Town, 7701 Rondebosch, South Africa*

<sup>2</sup>*Department of Mechanical Engineering, University of Cape Town, 7701 Rondebosch, South Africa*

October 7, 2021

## Abstract

Abstract here.

## 1 TODO

1. Get output parameters
2. Model automation
3. Mesh optimization

## 2 Introduction

=

- We will use: ton, mm, s, N, MPa, N-mm

### 2.1 Gas gun design

#### 2.1.1 title

## 3 Finite element model

A finite element model of the scenario is created to run computation experiments. Theses experiments provide data for the force and plastic deformation that the cap experiences as it makes contact with the transition piece. After several computational experiments are run, the resulting data is used to train a machine learning model that can predict the forces experienced by the cap without the need for a finite element model.

---

<sup>\*</sup>alhben001@myuct.ac.za

MASS	LENGTH	TIME	FORCE	STRESS	ENERGY	Steel Density	Steel Modulus	G - Gravity Constant
kg	m	s	N	Pa	Joule	7.83E+03	2.07E+11	9.81
kg	mm	ms	kN	Gpa	kN-mm	7.83E-06	2.07E+02	9.81E-03
g	cm	s	dyne	dyne/cm^2	erg	7.83E+00	2.07E+12	9.81E+02
g	cm	us	1e7N	Mbar	1e7 N-cm	7.83E+00	2.07E+00	9.81E-10
g	mm	s	1e-6N	Pa	1e-9 J	7.83E-03	2.07E+11	9.81E+03
g	mm	ms	N	Mpa	N-mm	7.83E-03	2.07E+05	9.81E-03
ton	mm	s	N	Mpa	N-mm	7.83E-09	2.07E+05	9.81E+03
lbf-s^2/in	in	s	lbf	psi	lbf-in	7.33E-04	3.00E+07	3.86E+02
slug	ft	s	lbf	psi	lbf-ft	1.52E+01	4.32E+09	32.2

Figure 1: Consistent units for ABAQUS . From <https://www.researchgate.net/post/What-are-the-Abaqus-Units-in-Visualization-units>

### 3.1 Geometry

Axial symmetry is used to reduce the problem to two dimensions. The resulting geometric model is presented in Figure 2. **Explain the model and the parts and geometries Table of geometric values**



Figure 2: Geometric model of two-stage gas gun pump tube.

### 3.2 Material models

The material models used for each component are presented here.

#### 3.2.1 High density polyethylene (HDPE)

High Density Polyethylene (HDPE) is modelled using the Ramberg-Osgood model as done so in the literature [2]. In 1D, the model is given by

$$E_c \varepsilon = \sigma + \alpha_c \sigma \left[ \frac{|\sigma|}{\sigma_{yc}} \right]^{n-1}, \quad (1)$$

where  $E_c$  is the Young's modulus,  $\alpha_c$  is the yield offset,  $\sigma_{yc}$  is the yield stress and  $n$  is the hardening exponent. In 3D, the model has the additional parameter of Poisson's ratio, denoted by  $\nu_c$ . The material parameters are determined by fitting the model to data from [2] using a **Python** script which can be found at [this link](#). Additionally, a 3D uniaxial ABAQUS simulation utilizing the model is compared to the 1D model (equation (1)) to verify that the model behaves as expected in ABAQUS . The results of the simulation, the behaviour of the model, and the data are displayed in Figure 3. The calibrated material parameters, as well as the other parameters required to define the model, are presented in Table 1.

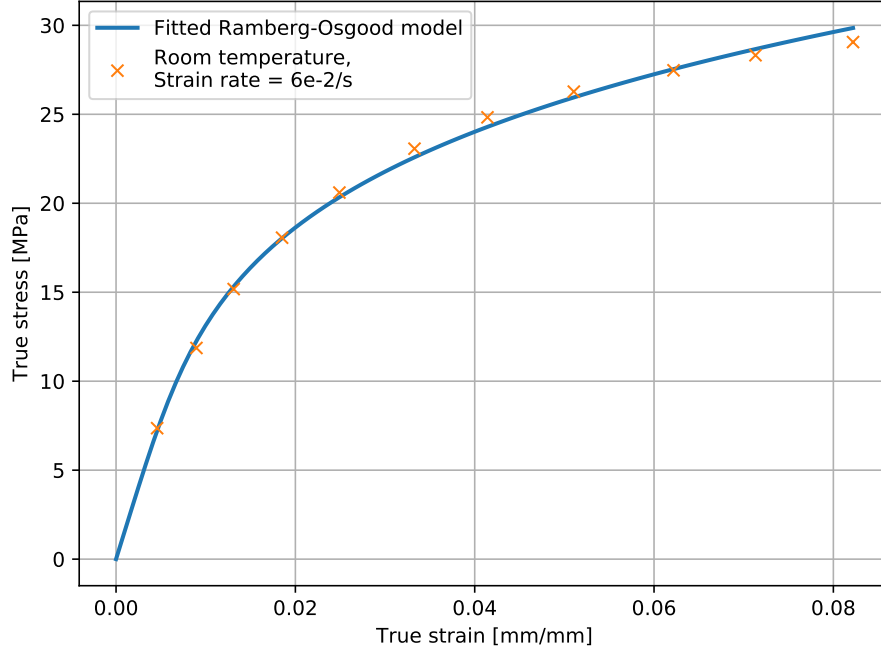


Figure 3: Stress-strain relation for HDPE modelled with the Ramberg-Osgood model. The model is calibrated to fit data from [2] (denoted by green 'x's). Additionally, the 1D model is compared to a uniaxial ABAQUS simulation using the calibrated material parameters. It is clear that the curves match each other and provide a good fit to the data.

Table 1: Material parameters for HDPE

Density ton/mm <sup>3</sup> [3, 2]	$\rho_c$	Young's modulus $E_c$ MPa	Poisson's ra- tio $\nu_c$ [7]	Yield stress $\sigma_{yc}$ MPa	Yield offset $\alpha_c$	Hardening exponent $n$
$0.95 \times 10^{-9}$		$1.63 \times 10^3$	0.46	14.6	0.342	4.26

### 3.2.2 Mild steel

The mild steel components are expected to remain in the elastic region and so only linear elastic material behaviour is considered. The material parameters are given in Table 2.

Table 2: Material parameters for mild steel Ref later

Density ton/mm <sup>3</sup>	$\rho_t$	Young's modulus $E_t$ MPa	Poisson's ra- tio $\nu_t$
$8 \times 10^{-9}$		$200 \times 10^3$	0.3

### 3.2.3 Aluminium

The aluminium components are expected to remain in the elastic region and so only linear elastic material behaviour is considered. The material parameters are given in Table 3.

Table 3: Material parameters for aluminium taken from [1]

Density $\rho_p$ ton/mm <sup>3</sup>	Young's modulus $E_p$ MPa	Poisson's ra- tio $\nu_p$
$2.69 \times 10^{-9}$	$68.3 \times 10^3$	0.34

### 3.3 Interactions

Contact interactions and tie constraints are applied between various parts in the assembly, see Figure 2. The relevant coefficients of friction for these interactions are obtained from the literature and summarised in Table 4.

Table 4: Relevant coefficients of friction for problem

HDPE on steel $\mu_{cs}$ [6]	steel on steel $\mu_{ss}$ [8]	aluminium on steel $\mu_{as}$ [5]
0.25	0.2	0.5

The cap is assigned a contact interaction with the pump tube and the transition piece. Hard contact is used to describe the normal behaviour and sliding friction is used to describe the tangential behaviour with a coefficient of friction of  $\mu_{cs}$ , see Table 4. The piston is similarly assigned a contact interaction with the pump tube with a coefficient of friction of  $\mu_{as}$ .

The pump tube is tied to the transition piece to approximate the threaded interaction. Additionally, a tie constraint is assigned between the cap and the piston. The interaction between the cap and piston would likely better be described by cohesive interaction. However, the interaction between the cap and the piston is expected to have little influence on the results of interest from the model, and so a tie constraint is used as a convenient first approximation.

### 3.4 Initial and boundary conditions

1. Region A and B are encastrated
2. The piston and end cap are assigned an initial velocity of  $v_0$
3. A pressure load is applied to the back of the piston with varying magnitude throughout time.
4. A pressure load is applied to the front of the cap with varying magnitude throughout time.

### 3.5 Time integration

An implicit Newmark-method is used with time increments of  $\Delta t$

### 3.6 Variable input parameters and desired output parameters

Input parameters to be varied:

1.  $v_0$
2.  $p_{\text{back}}$
3.  $p_{\text{front}}$

Outputs of interest:

1.  $v$
2.  $x_t$
3.  $\langle \Phi_c \rangle$
4.  $\Delta p$
5. Piston in contact
6. Deformation elastoplastic

Outputs to later be predicted:

1.  $F_c$
2.  $\langle \dot{\Phi}_c \rangle$
3. Piston in contact
4. Deformation elastoplastic

### 3.7 Single test simulation

#### 3.7.1 Machine learning surrogate model

Loading regime classification

### 3.8 Mesh optimization

Parameters

1. ratio of element expansion for piston
2. ratio of element expansion for tube
3. n elements

Objective function

1. Min elements

Constraint

1. Force
2. Dissipation

## 4 Machine learning surrogate model

### 4.1 Feature engineering

Predictive features:

1. Coefficient of friction:  $\mu$

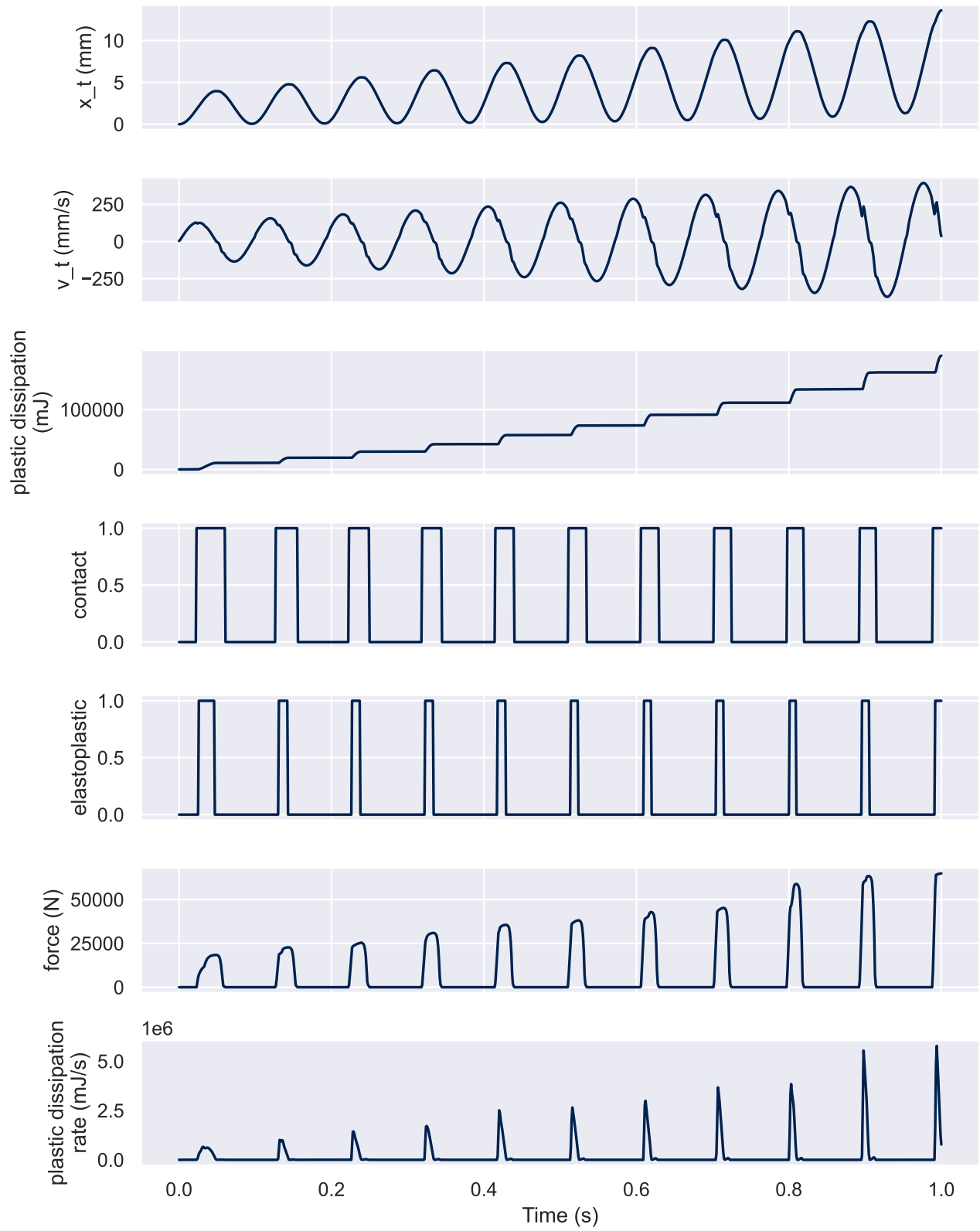


Figure 4: Loading vs time.

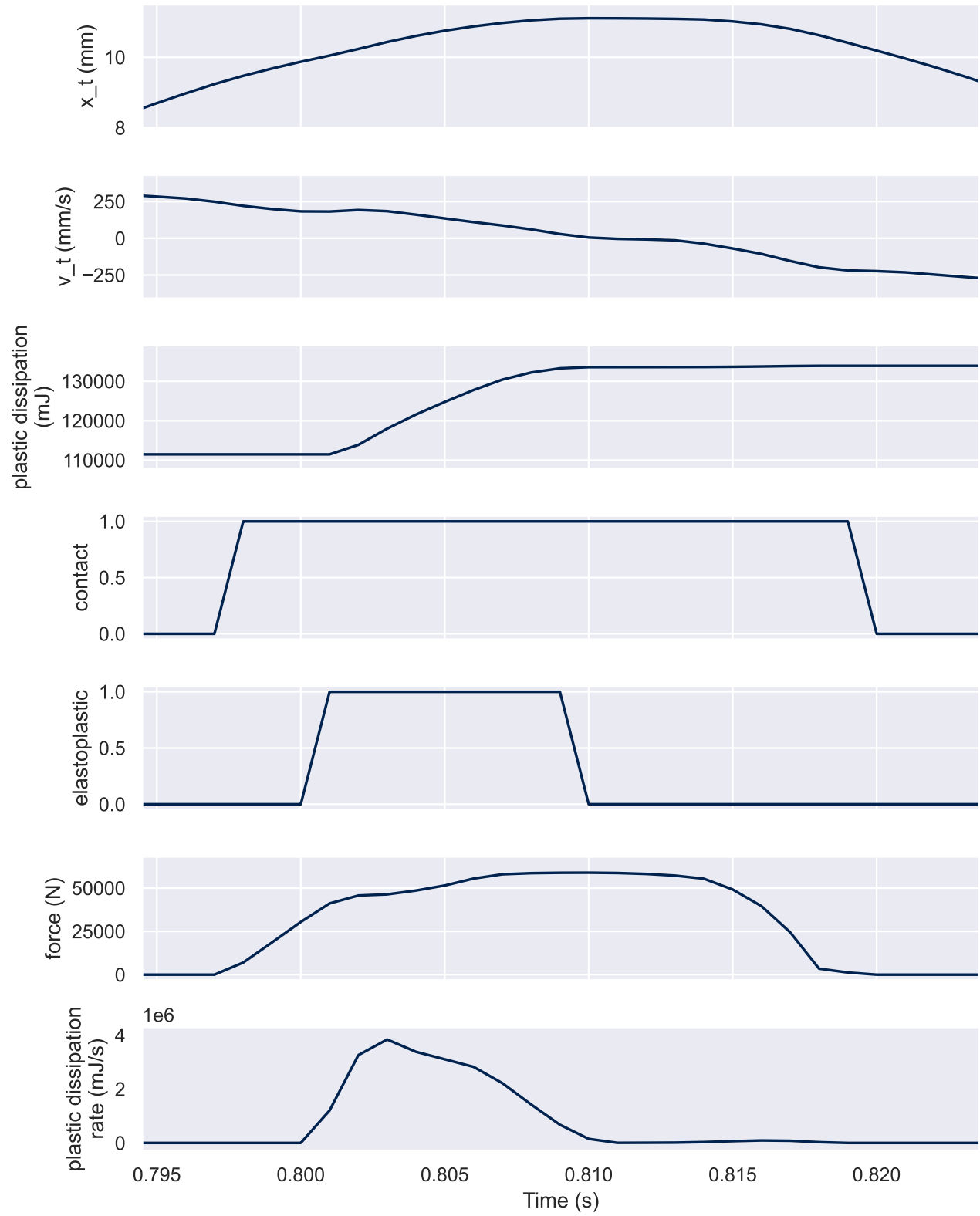


Figure 5: Loading vs time zoom.

2. Taper angle:  $\alpha$

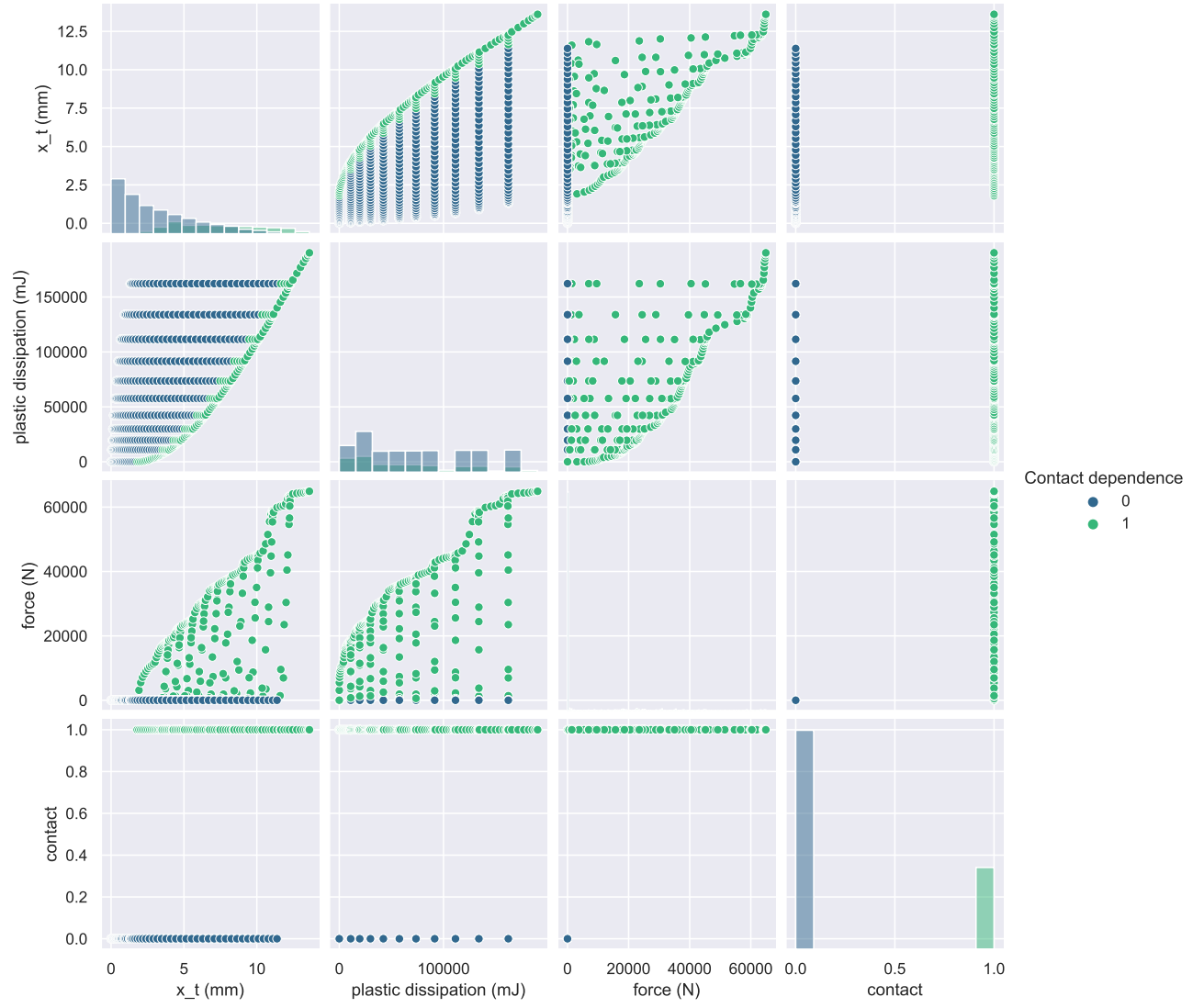


Figure 6: Contact dependence.

3. Velocity:  $v$
4. Distance between piston front and taper start:  $x_{taper}$
5. Pressure difference between piston front and back:  $\Delta p$
6. Piston length:  $l_p$
7. Piston density:  $\rho_p$
8. Accumulative plastic strain in the piston:  $\gamma$

Dependent variables:

1. Axial force on piston due to taper:  $F_z$
2. Increment in accumulated plastic dissipation:  $\Delta \gamma$



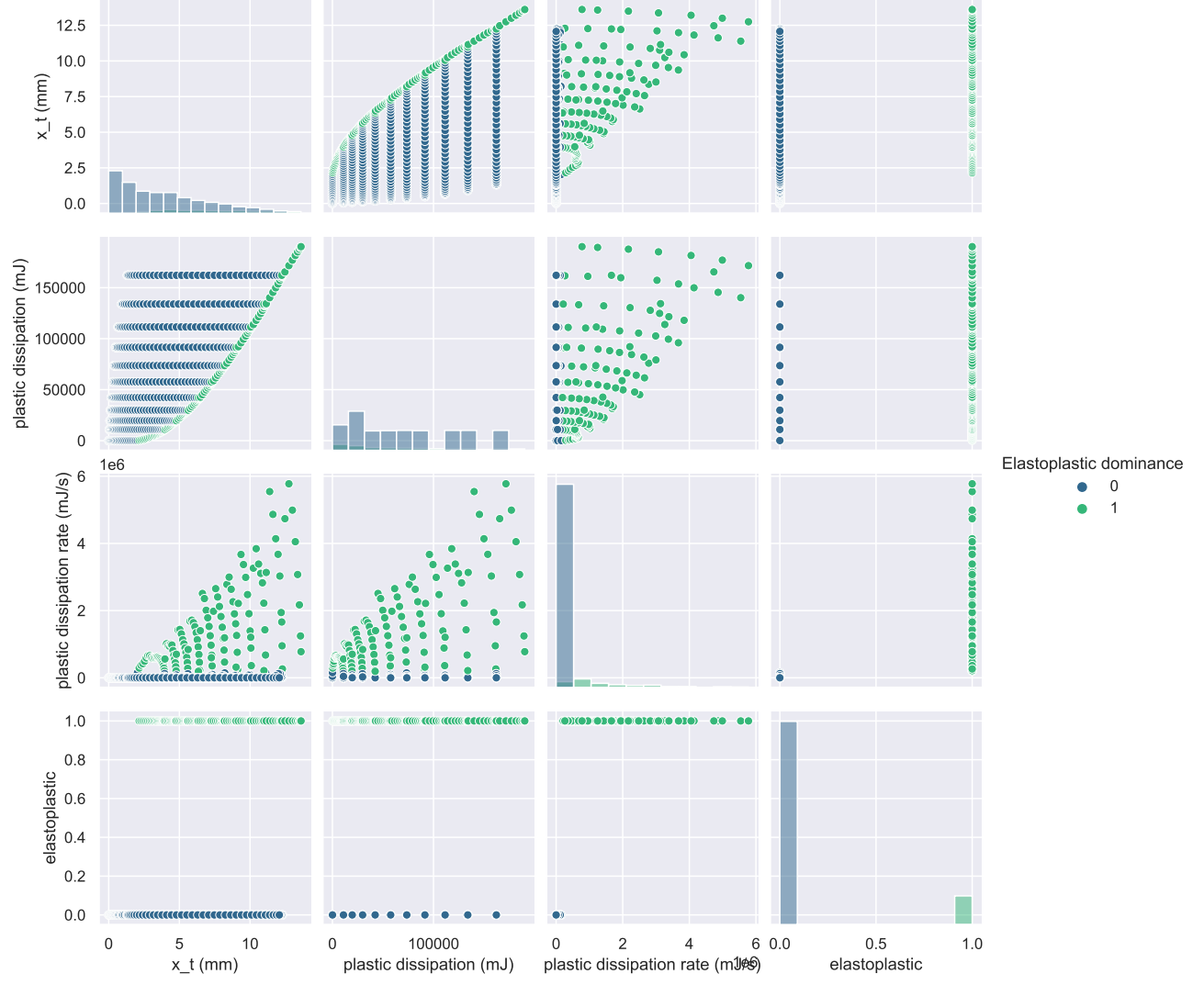


Figure 7: Elastoplastic dependence.

#### 4.1.1 Dimensional analysis

Table 5: Fundamental dimensional units

Mass $[M]$	Length $[L]$	Time $[T]$
------------	--------------	------------

$$\Pi = F_c^{k_1} \langle \dot{\Phi}_c \rangle^{k_2} \Delta P^{k_4} v^{k_5} \langle \Phi_c \rangle^{k_3} x_t^{k_6} \quad (2)$$

$$r = 3 \quad (3)$$

$$n = 24 \quad (4)$$

$$n_{\text{n-dim}} = n - r = 21 \quad (5)$$

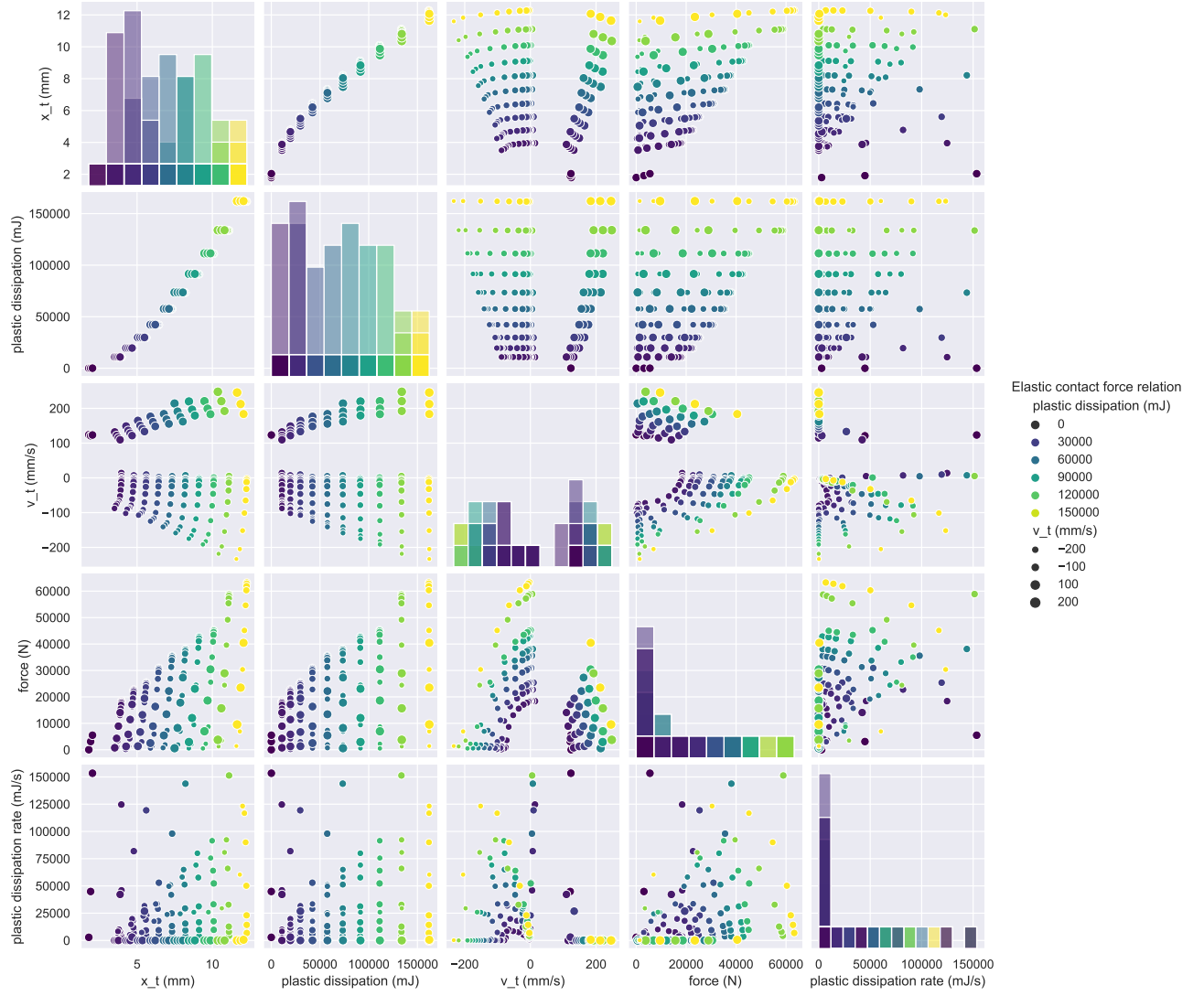


Figure 8: Contact elastic force.

$$\begin{matrix} M \\ L \\ T \end{matrix} \begin{matrix} F_c & \langle \Phi_c \rangle & \Delta P & v & \langle \Phi_c \rangle & x_t \end{matrix} \begin{bmatrix} 1 & 1 & 1 & 0 & 1 & 0 \\ 1 & -1 & -1 & 1 & -1 & 1 \\ -2 & -3 & -2 & -1 & -2 & 0 \end{bmatrix} \begin{bmatrix} k_1 \\ k_2 \\ k_3 \\ k_4 \\ k_5 \\ k_6 \end{bmatrix} = \mathbf{0}. \quad (6)$$

1. Enter units as symbols in sympy
2. Construct dimensional matrix
3. Find solutions  $k_i^j$  to dimensional matrix by  $n - r$  values in  $k$  to 0 (except for 1 which on sets to 1).
4. Automatically print out resulting dimensionless products table.

Based on [4]:

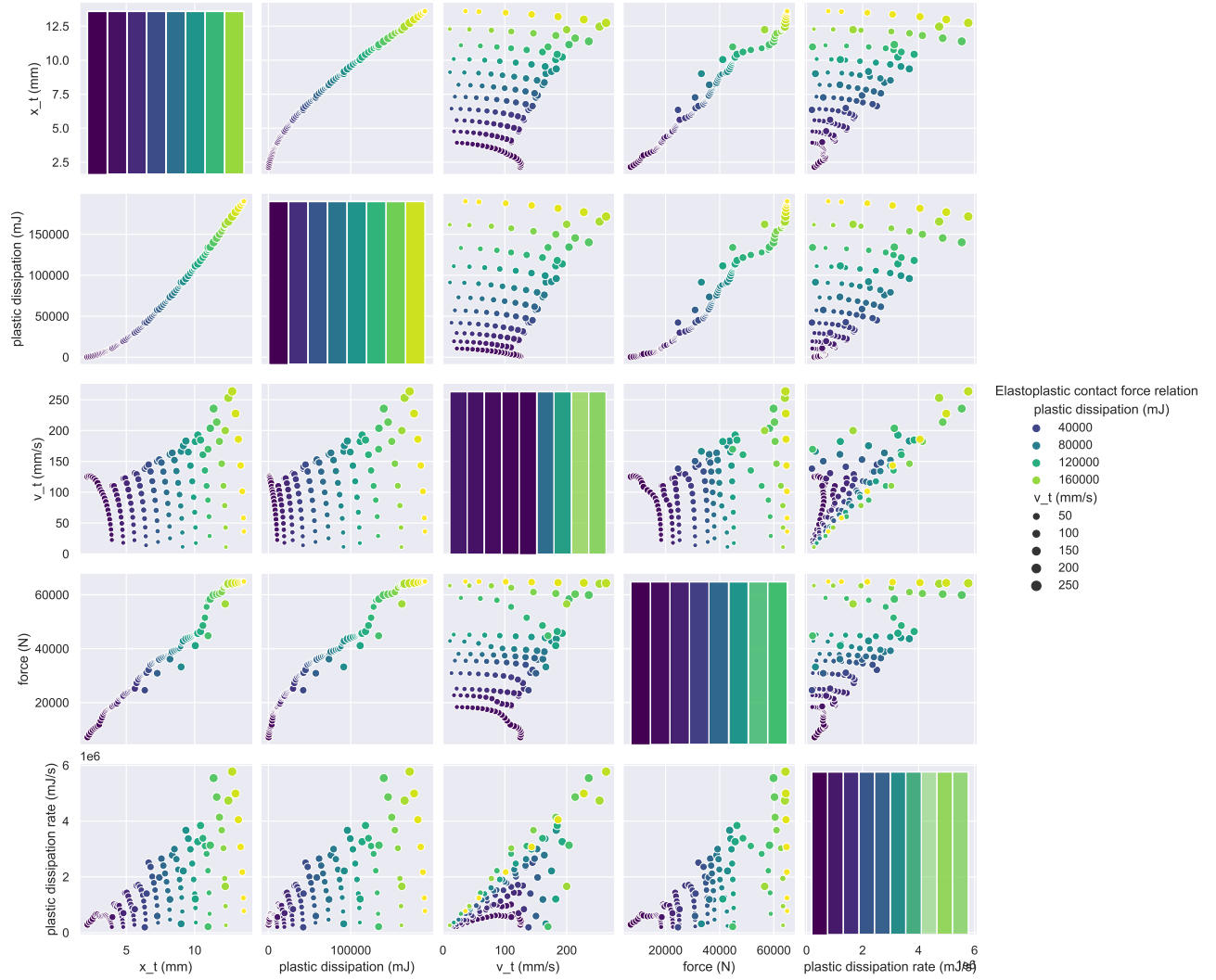


Figure 9: Contact elastoplastic force.

Notes:

1.

Direct quote from [4]

“Dimensional analysis is a method with the aid of which one may for instance test a formula for dimensional correctness. It leads to a first understanding of the solution of a physical problem and yields a precise information about the number of variables that are necessary to describe it, a fact that is particularly important when experiments are being performed. Very often dimensional analysis reduces the number of variables upon which a physical problem was initially surmised to depend. If for instance the quantity  $y$  depends upon  $x_1, x_2, \dots, x_n$ , where all quantities have a certain physical dimension, then dimensional analysis shows that  $y$  can only depend upon certain products of powers of  $x_1, x_2, \dots, x_n$ , a fact that corresponds regularly to a considerable reduction of the number of variables. Naturally then, experiments may more simply or more economically be performed than without knowledge of this fact.”

“The first step in a dimensional analysis consists in the listing of the parameters, which influence a physical problem. This step is very decisive. If too many variables are listed that may describe a

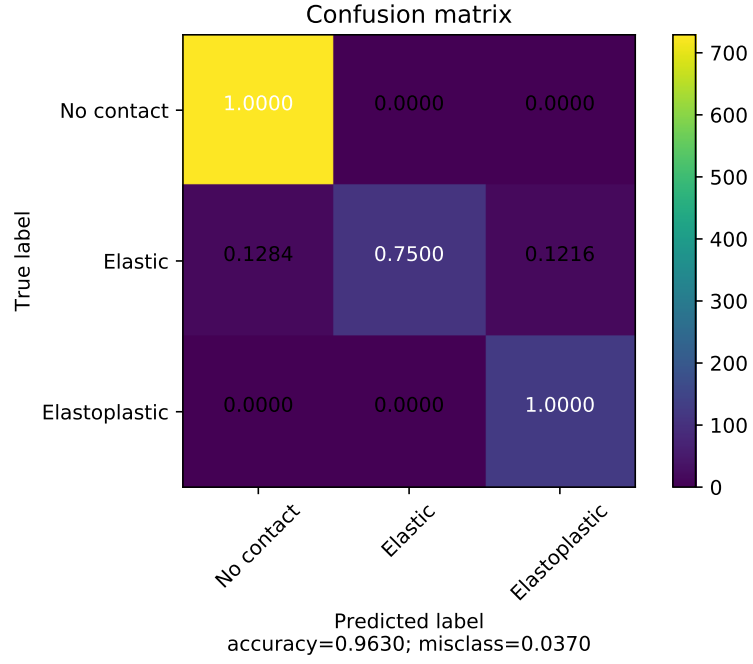


Figure 10: Confusion matrix of loading regime classification

physical problem, then the final equations will contain superfluous variables, if too few variables are introduced, incomplete equations may emerge, which results in incomplete equations or "more often" false inferences or the result can not be expressed in terms of dimensionally homogeneous functions."

## 4.2 Experimental input parameters

In order of importance:

1. Initial velocity:  $v_0$
2. Pressure path:  $p_{path}$
3. Piston length:  $l_p$
4. Coefficient of friction:  $\mu$

Table 6: Variables on which the problem depends Check that units are correct

Component	Description	Symbol	Units
Cap	Axial contact force	$F_c$	$[MLT^{-2}]$
	Rate of volume average plastic dissipation	$\langle \dot{\Phi}_c \rangle$	$[ML^{-1}T^{-3}]$
	Volume average plastic dissipation	$\langle \Phi_c \rangle$	$[ML^{-1}T^{-2}]$
	Pressure difference	$\Delta P$	$[ML^{-1}T^{-2}]$
	Velocity	$v$	$[LT^{-1}]$
	Distance of cap past taper	$x_t$	$[L]$
	Length past piston	$l_c$	$[L]$
	Diameter	$d_c$	$[L]$
	Density	$\rho_c$	$[ML^{-3}]$
	Young's modulus	$E_c$	$[ML^{-1}T^{-2}]$
	Poisson's ratio	$\nu_c$	$[\bullet]$
	Yield stress	$\sigma_{yc}$	$[ML^{-1}T^{-2}]$
Piston	Length	$l_p$	$[L]$
	Diameter	$d_p$	$[L]$
	Density	$\rho_p$	$[ML^{-3}]$
	Young's modulus	$E_p$	$[ML^{-1}T^{-2}]$
	Poisson's ratio	$\nu_p$	$[\bullet]$
Transition piece	Length	$l_t$	$[L]$
	Diameter change	$\Delta d_t$	$[L]$
	Density	$\rho_t$	$[ML^{-3}]$
	Young's modulus	$E_t$	$[ML^{-1}T^{-2}]$
	Poisson's ratio	$\nu_t$	$[\bullet]$
Friction	Cap-on-steel CoF	$\mu_{cs}$	$[\bullet]$
	Steel-on-steel CoF	$\mu_{ss}$	$[\bullet]$
	Aluminium-on-steel CoF	$\mu_{as}$	$[\bullet]$

Table 7: Non-dimensional parameters

$$\begin{array}{cccccc}
F_c & \langle \dot{\Phi}_c \rangle & \langle \Phi_c \rangle & \Delta P & v & x_t \\
k_1 & k_2 & k_3 & k_4 & k_5 & k_6
\end{array}$$

### 4.3 Experimental results

### 4.4 Model

## 5 Packaging of model for use in 1D code

### 5.1 PIP

### 5.2 Usage example

## References

- [1] *Aluminium: Specifications, Properties, Classifications and Classes*. URL: <https://www.azom.com/article.aspx?ArticleID=2863>.
- [2] M. Amjadi and A. Fatemi. “Tensile behavior of high-density polyethylene including the effects of processing technique, thickness, temperature, and strain rate”. *Polymers* 12.9 (2020), p. 1857.
- [3] A. Dasari, S. Duncan, and R. Misra. “Microstructural aspects of tensile deformation of high density polyethylene”. *Materials science and technology* 19.2 (2003), pp. 244–252.
- [4] K. Hutter and K. Jöhnk. *Continuum Methods of Physical Modeling: Continuum Mechanics, Dimensional Analysis, Turbulence*. Springer Science & Business Media, 2013.
- [5] M. Javadi and M. Tajdari. “Experimental investigation of the friction coefficient between aluminium and steel”. *Materials Science-Poland* 24.2/1 (2006), pp. 305–310.
- [6] M. E. Kinsella, B. Lilly, B. E. Gardner, and N. J. Jacobs. “Experimental determination of friction coefficients between thermoplastics and rapid tooled injection mold materials”. *Rapid Prototyping Journal* (2005).
- [7] K.-h. Nitta and M. Yamana. *Poisson’s ratio and mechanical nonlinearity under tensile deformation in crystalline polymers*. InTech Rijeka, 2012.
- [8] T. Trzepieciniski. “A study of the coefficient of friction in steel sheets forming”. *Metals* 9.9 (2019), p. 988.